Astron. Astrophys. 266, 501–512 (1992)

ASTRONOMY AND ASTROPHYSICS

Radiative transfer for transiently heated particles

R. Siebenmorgen [1], E. Krügel [2], and J.S. Mathis [3]

[1] European Southern Observatory, Karl-Schwarzschild-Str. 2, W-8046 Garching bei München, Federal Republic of Germany
[2] Max-Planck-Institut für Radioastronomie, Auf dem Hügel 69, W-5300 Bonn 1, Federal Republic of Germany
[3] Washburn Observatory, University of Wisconsin-Madison, 475 North Charter Street, Madison, WI 53707, USA

Received May 9, accepted July 25, 1992

Abstract. (1) We discuss different methods for calculating the emission of transiently heated small grains (sizes a < 100 Å) and of polycyclic aromatic hydrocarbons (PAHs). We present their temperature distribution functions and spectra in various environments and give practical advice how to best calculate them. We demonstrate that current treatments gravely underestimate the submm part of the spectrum. (2) We investigate under which conditions very small silicate grains of 5–80 Å radius could be detected by their 9.7 μm emission feature. From the absence of such a feature in reflection nebulae we estimate an abundance in this component of less than 5% of the total silicate abundance. (3) We present for the first time spectra of PAH features in media with high optical depth obtained from self-consistent radiative transfer calculations. As an application we analyze spectra of globules by simulating the observational procedure of beam switching. We demonstrate that extended emission from globules in the 12 and 25 μm IRAS bands can be explained by PAH and small graphite emission.

Key words: dust – infrared emission

1. Introduction

The time variable emission of very small grains is frequently observed and seen in many diverse sources. It becomes important whenever the dusty medium is penetrated by UV photons. Then the spectrum acquires a broad shoulder in the mid IR (5 to 20 μm) and resonances from PAHs appear as the "Unidentified Infrared Bands" as has been amply demonstrated observationally (Aitken 1981; Sellgren 1984; Boulanger & Perault 1988; Siebenmorgen & Krügel 1992; henceforth SK). Together with an improved understanding of the physical properties of very small grains (Allamandola et al. 1989; Puget & Leger 1989) numerical methods have been devised to quantitatively calculate their emission (Duley 1973; Greenberg & Hong 1974; Purcell 1976; Aannestad & Kenyon 1979; Draine & Anderson 1985; Desert et al. 1986; Dwek 1986). More recently a powerful technique was presented by Guharthakurta & Draine (1989; henceforth GD). In this paper we have four goals. (i) The emission of very small particles is an intrinsically difficult process, in contrast to the time-constant radiation from big grains which is described by just the dust temperature and the corresponding Planck function. Therefore we give a guideline in the form of illustrative figures how very small grains emit in various environments for those who do not wish to perform the underlying calculations, but need crude estimates. (ii) We give practical recommendations for those who actually want to calculate the emission from very small grains. This may be useful in the computational struggle, although the basic algorithms are already in the literature. (iii) As an application, we investigate how one may detect silicate grains with diameters of a few tens of Angstrom. As similarly tiny carbon particles are directly observed in the form of PAHs there is no reason why the lower limit in the size distribution of silicates should be much higher than 10 Å. (iv) Finally, we incorporate very small grains into a program of radiative transfer including the treatment of scattering. It is designed for spherical symmetry and we apply it to isolated globules without embedded young stars that are heated only by an outer radiation field. We demonstrate how dramatically their presence changes the IR appearance of these objects.

Send offprint requests to: R. Siebenmorgen

2. Calculating the emission from grains with temperature fluctuations

2.1. When must very small grains be considered?

Calculating the emission of a particle with temperature fluctuations is considerably more complicated and time consuming than of a grain in temperature equilibrium. Therefore it is useful to know when such calculations are necessary at all and how they be best performed. Generally speaking, they should be applied whenever the time interval between the absorption of photons with an energy $h\nu$ comparable to the enthalpy of the grain is much longer than the cooling time of the grain. This is, however, not a very practical advice and it is more instructive to show for typical cases how temperature fluctuations modify the spectrum.

Let $P(T)$ be the normalized density probability,

$$\int P(T)\,\mathrm{d}T = 1,$$

so that $P(T)\,\mathrm{d}T$ gives the probability for finding a grain in the temperature interval from $T \ldots T + \mathrm{d}T$. For very large grains $P(T)$ approaches a δ-function. Their temperature fluctuates very little around an equilibrium value T_{eq}. It is determined from the energy balance between emission and absorption,

$$4\pi \int K_\nu J_\nu \,\mathrm{d}\nu = 4\pi \int K_\nu B_\nu(T_{\mathrm{eq}})\,\mathrm{d}\nu, \qquad (1)$$

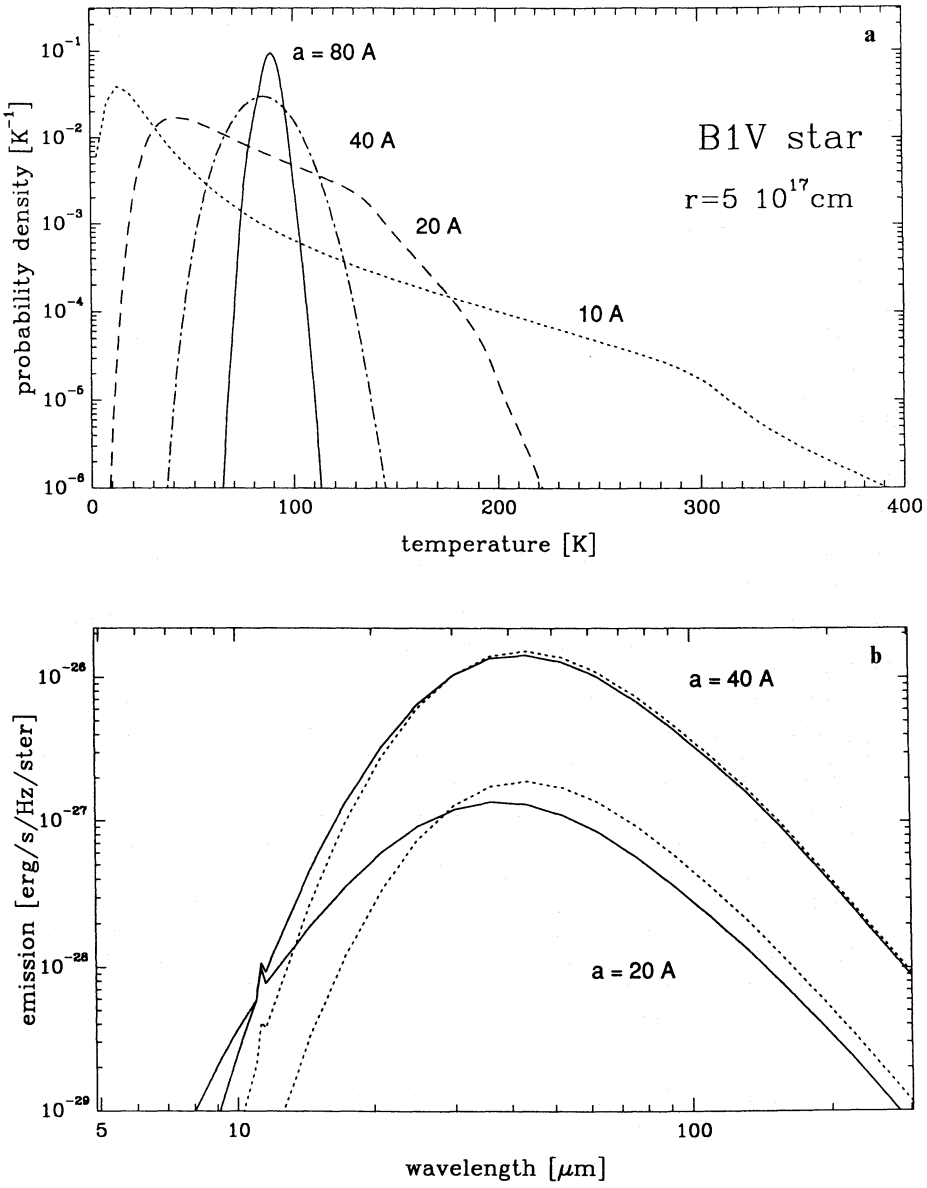

Fig. 1. a The probability function $P(T)$ for graphite grains with radii from 10 to 80 Å at a distance of $5\ 10^{17}$ cm from a B1V star with $L = 10^4 L_\odot$ and $T_\star = 2\ 10^4$ K. $P(T)$ gives the probability for finding a grain in the temperature interval from $T \ldots T+1$ K. **b** The emission of such grains with 20 and 40 Å radius calculated after Eqs. (1) and (2) assuming an equilibrium temperature T_{eq} (dashed curves) and after Eqs. (3) and (4) where allowance is made for temperature fluctuations (solid)

which holds at any time. J_ν denotes the mean intensity, B_ν the Planck function and K_ν the absorption coefficient. The radiation of the grain is given by

$$\varepsilon_\nu = K_\nu\ B_\nu(T_{eq}) \qquad (2)$$

Small grains do not attain a steady state temperature. Their energy content is time-variable and $P(T)$ describes in an adequate way these fluctuations. The emission of such a grain in a radiation field J_ν is calculated, once $P(T)$ is known, from

$$\varepsilon_\nu = K_\nu \int B_\nu(T)\ P(T)\ \mathrm{d}T \qquad (3)$$

Now one needs to know not only the optical properties (dielectric functions) of the grain, but also its thermal behavior as it determines the cooling rate. Whenever the function $P(T)$ is narrow one may use Eq. (2). If, however, $P(T)$ is broad Eq. (3) must be applied even if $P(T)$ attains its maximum at a value T_{max} close to T_{eq}. The use of Eq. (3) becomes necessary if one or a combination of the following effects is at work:

(*a*) *The grains are small.* We show for two environments how $P(T)$ broadens with decreasing grain size. The subsequent Figs. 1–7 refer to graphite grains. In Fig. 1 a we choose a typical location in a reflection nebula at a distance of $r = 5\ 10^{17}$ cm from a B1V star with $L = 10^4 L_\odot$ and $T_{eff} = 20000$ K. The star is assumed to radiate as a black body. The grain radii a vary from 10 and 80 Å. For the largest grains ($a = 80$ Å) the probability density is a narrow function and its equilibrium temperature T_{eq} of 87.4 K equals within 0.2 K the value T_{max}, where $P(T)$ has its maximum. Therefore the emission of such a grain is perfectly evaluated from Eq. (2). Calculating $P(T)$ for grains that show only slight temperature fluctuations is not only unnecessary, but can also be numerically difficult because $P(T)$ changes so rapidly. If the particle radius in Fig. 1 is only 40 Å the results from Eq. (2) and (3) are still very similar and only at wavelengths below 20 μm do the few temperature excursions of the fluctuating grain lead to a stronger radiation (Fig. 1 b). When $a = 20$ Å or smaller $P(T)$ falls off very gradually and Eq. (2) must be abandoned. There is now a

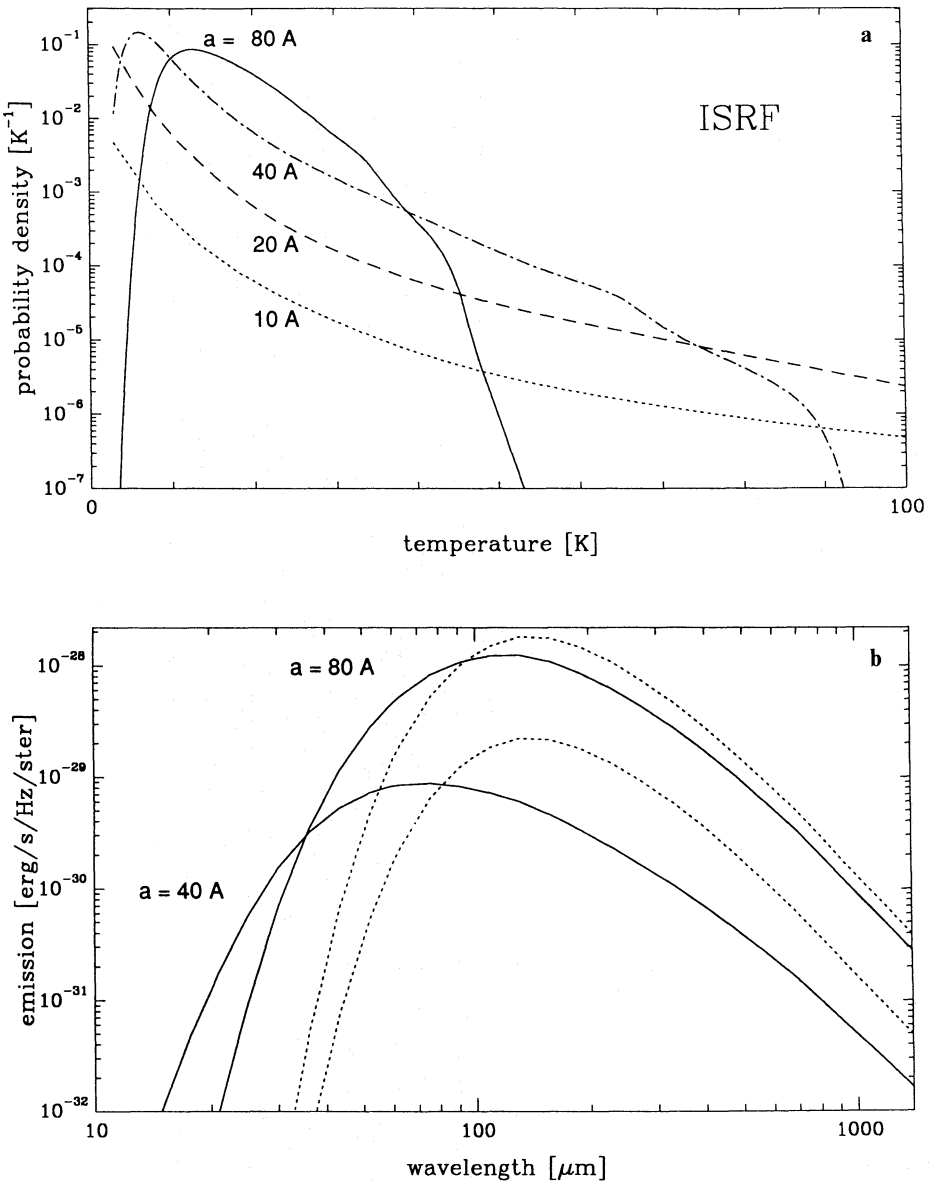

Fig. 2. **a** Same as Fig. 1a, but the grains are now in the interstellar radiation field in the vicinity of the sun. **b** Same as Fig. 1b, but for grain radii of 40 and 80 Å

non-negligible chance of finding a grain at a temperature far away from T_{max} and it is exactly this behavior which leads to color temperatures in the spectrum that are much higher than the time-averaged temperature of the bulk material.

(*b*) *The radiation field is weak.* If the environment is changed from a reflection nebula to the vicinity of the sun, where J_ν is given by the interstellar radiation field (ISRF), temperature fluctuations become dramatically more important. This can be understood from plots of $P(T)$: Because of the relative scarceness of energetic photons the grains now stay for long spells at very low temperatures and the probability density peaks there. The decline of $P(T)$ towards higher temperatures is then very gradual. Equation (2) yields vastly different results from Eq. (3) even for grains with $a = 80$ Å. Figure 3 demonstrates how the weakening of the radiation field influences the probability density and the spectra; we have chosen a grain of $a = 40$ Å at distances from a B1V star between $5\ 10^{16}$ to $5\ 10^{19}$ cm. Obviously, Eq. (2) is not applicable if the grain is much further away than $5\ 10^{17}$ cm.

(*c*) *The radiation field is hard.* Finally, we demonstrate the effect of hardness of the impinging radiation field. The graphite particles considered so far do not possess a threshold energy necessary for their excitation. This is different for PAHs which are believed to require, at least, visual photons for stimulating their IR resonances. Again we consider a source with $L = 10^4\ L_\odot$, but this time we change the stellar radiation field from a black body of 20000 K, corresponding to the effective temperature of a B1V star, to black bodies of 2000 and 200 K, respectively, while keeping the total flux [erg s^{-1} cm^{-2}] constant. 2000 K would be appropriate for a hot, optically thick dust cocoon around the star as it may form in an infalling envelope with a $\varrho \propto r^{-1.5}$ density distribution. A radiation temperature of $T = 200$ K may be realized if the star is enveloped by a thick shell of high visual extinction, for example like W3(OH) (Chini et al. 1986). For lower radiation temperatures the photons impinge at a higher rate while each photon carries on the average less energy. The probability function consequently narrows and temperature excursions become less important. This is illustrated in Figs. 4 and 5 for grains with 40 and 10 Å radius.

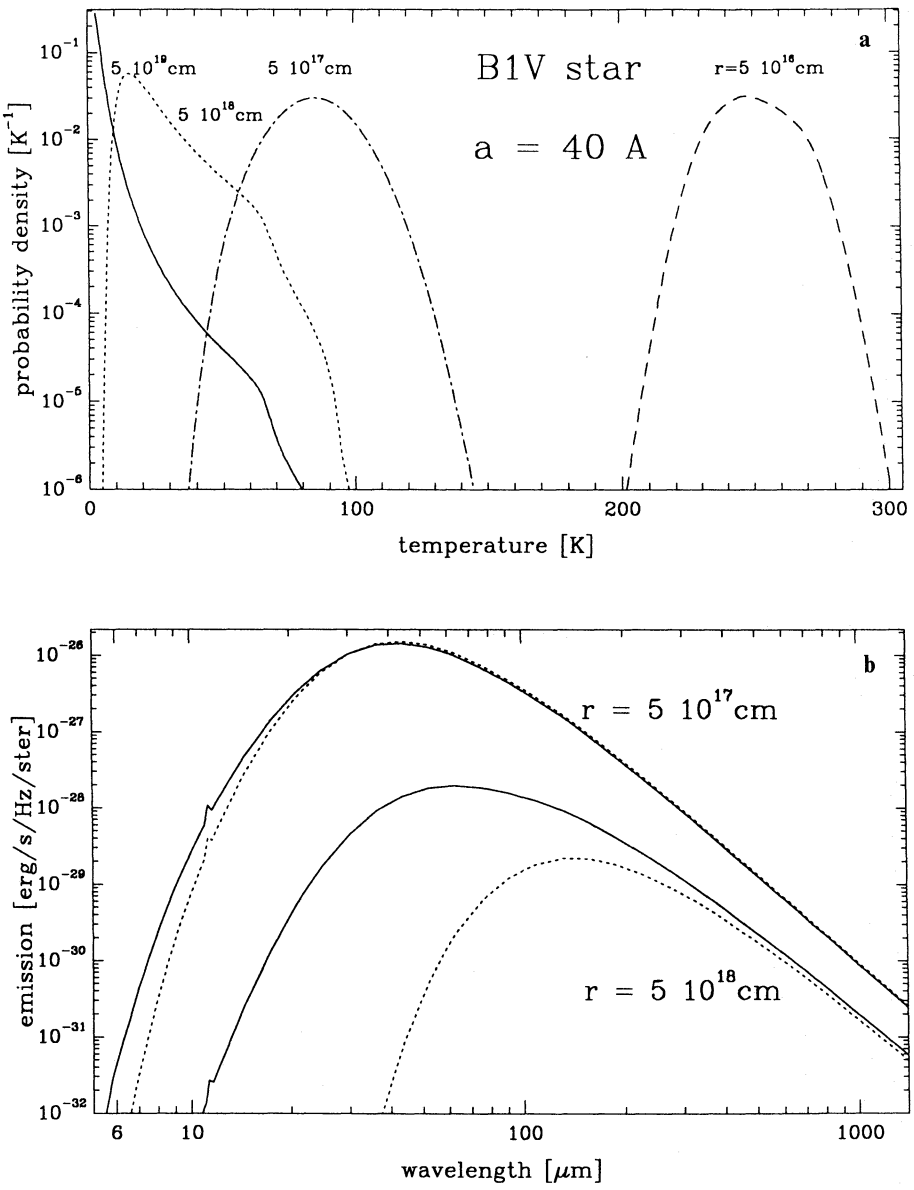

Fig. 3. **a** $P(T)$ for graphite grains of 40 Å radius positioned at distances between $5\,10^{16}$ to $5\,10^{19}$ cm from a B1V star. With increasing distance the curves are shifted to the left. **b** The resulting spectra for distances of $5\,10^{17}$ and $5\,10^{18}$ cm calculated with temperature fluctuations (solid) and without them (dashed).

The smaller particles with ($a = 10$ Å) fluctuate strongly even in a 2000 K black body radiation field so that the resulting spectrum is very different from the equilibrium case.

2.2. *Methods of calculating temperature fluctuations*

An efficient method was presented by GD. As each absorption or emission process corresponds to a transition in the enthalpy U of the grain from an initial state i to a final state f they define a matrix whose elements A_{fi} denote the probability for such a transition per unit time. The probability P_i (see Eq. 3) for finding a randomly picked grain in the enthalpy state i is determined from the balance for the population of each level f

$$\sum_{i \neq f} A_{fi} P_i - P_f \sum_{k \neq f} A_{kf} = 0 \qquad (4)$$

If the matrix element A_{fi} refers to photon absorption ($i < f$) it is given by $J_\nu K_\nu \Delta\nu/h\nu$. In the case of emission ($i > f$) $A_{fi} = B_\nu(T_i)\, K_\nu\, \Delta\nu/h\nu$, where T_i is the temperature of the grain in the initial state i. $h\nu = |U_i - U_f|$ is the energetic difference between initial and final state and $h\,\Delta\nu$ denotes the width of the initial enthalpy interval. GD achieve a great numerical advantage by assuming that emission from any state i occurs only to the next lower state $i-1$, however, with a probability that is the sum over all possible downward transitions: $A_{i-1,i} = \int B_\nu(T_i)\, K_\nu\, \mathrm{d}\nu/h\nu$. In this way, they obtain a matrix whose elements A_{fi} for emission, which are located above the main diagonal, are all zero except those just above the main diagonal. Equation (4) can then be solved very rapidly. Because this method neglects higher order transitions that obviously would occur in a real grain, say from i to $f = i-3$, it is useful to compare the spectrum obtained when all downward transitions are allowed with the one incorporating the assumption $A_{fi} = 0$ for $f < i-1$. To maximize possible discrepancies between both methods we choose a very small grain ($a = 5$ Å) at a distance of $5\,10^{17}$ cm from a B1V star. We see in Fig. 6, calculated with 400 enthalpy bins, that the spectral agreement at $\lambda < 30\,\mu$m is very good. Also the total integral under the two curves is within 1% the same. However, at

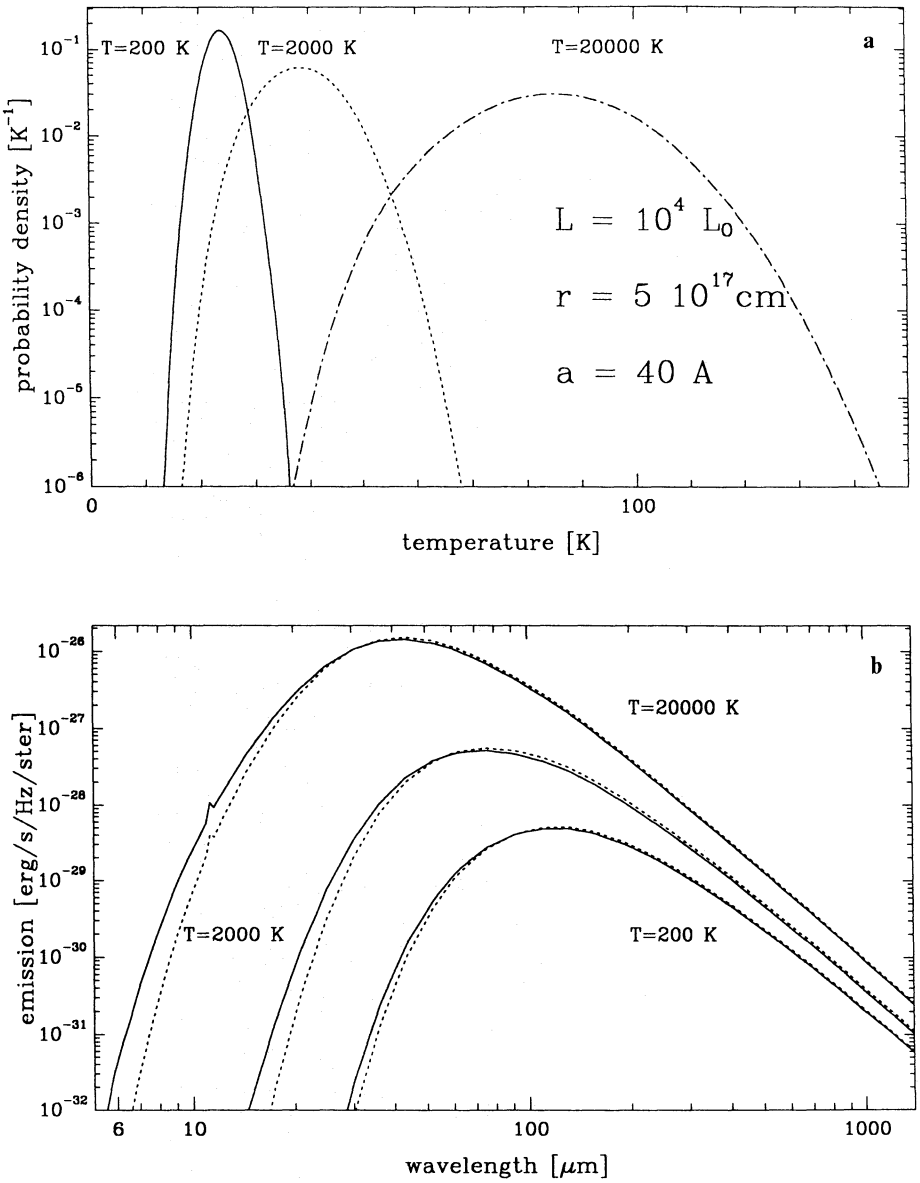

Fig. 4. **a** A graphite grain of 40 Å radius at a distance of 5 10^{17} cm from a source with $10^4 L_\odot$ emitting Planck spectra of 200, 2000 and 20000 K. **b** The resulting spectra in the approximation of Eqs. (1) and (2) (dashed) and calculated after Eqs. (3) and (4) (solid)

wavelengths $>30\,\mu$m the full matrix gives substantially higher fluxes. This can be understood by comparing the probability densities. In the low temperature range (<100 K) some transitions jumping over several enthalpy bins occur which are not accounted for by the GD approximation, which may therefore grossly underestimate the emission at submm wavelengths. The methods which allows $A_{if} \neq 0$ for $f < i-1$, although more exact, has the disadvantage that in order to calculate $P(T)$ a full inversion of a large matrix is necessary, which becomes too cumbersome for radiative transport codes.

Even when using the efficient method of GD, for radiative transport calculations one has to properly select the enthalpy bins. As $P(T)$ varies strongly with harshness and strength of the radiation field as well as with particle size a reasonable grid is sometimes hard to find. The boundaries of the grid, say $U_{\min}$ and $U_{\max}$, are hard to determine beforehand and intuitive values like $U_{\min} = 0$ and $U_{\max} = h\nu_{\max}$ are often not adequate. They should therefore be iterated: Starting with a first choice that crudely brackets the maximum of $P(T)$ one can find a better adapted grid by using as new boundaries those values of T where $P(T)$ has dropped by some factor (for instance, 10^{12}) from its maximum. Considerations of computing time make it mandatory to restrict the number of enthalpy intervals to a minimum. This, of course, must not be done at an undue expense of accuracy. A useful, but not very precise indicator (see Fig. 7) for accuracy is the time averaged ratio of emitted over absorbed energy, which should, of course be one. Generally, a grid of one hundred enthalpy bins is sufficient provided they are properly selected. For higher demands in accuracy one may have to use up to 500 grid points. The simplest grid is that of constant mesh size, either in temperature or enthalpy. In our experience it is generally advisable to keep the width of the temperature intervals $\Delta T = \text{const}$. Such a grid has at low temperatures a finer spacing in enthalpy ($U \propto T^{2\ldots3}$) and therefore better handles the far IR photons of low energy (Fig. 7). In the limit of very small mesh size the results from the two grids must of course converge.

Another method to calculate the emission spectrum of a grain with temperature fluctuations is to follow the time evolution of the

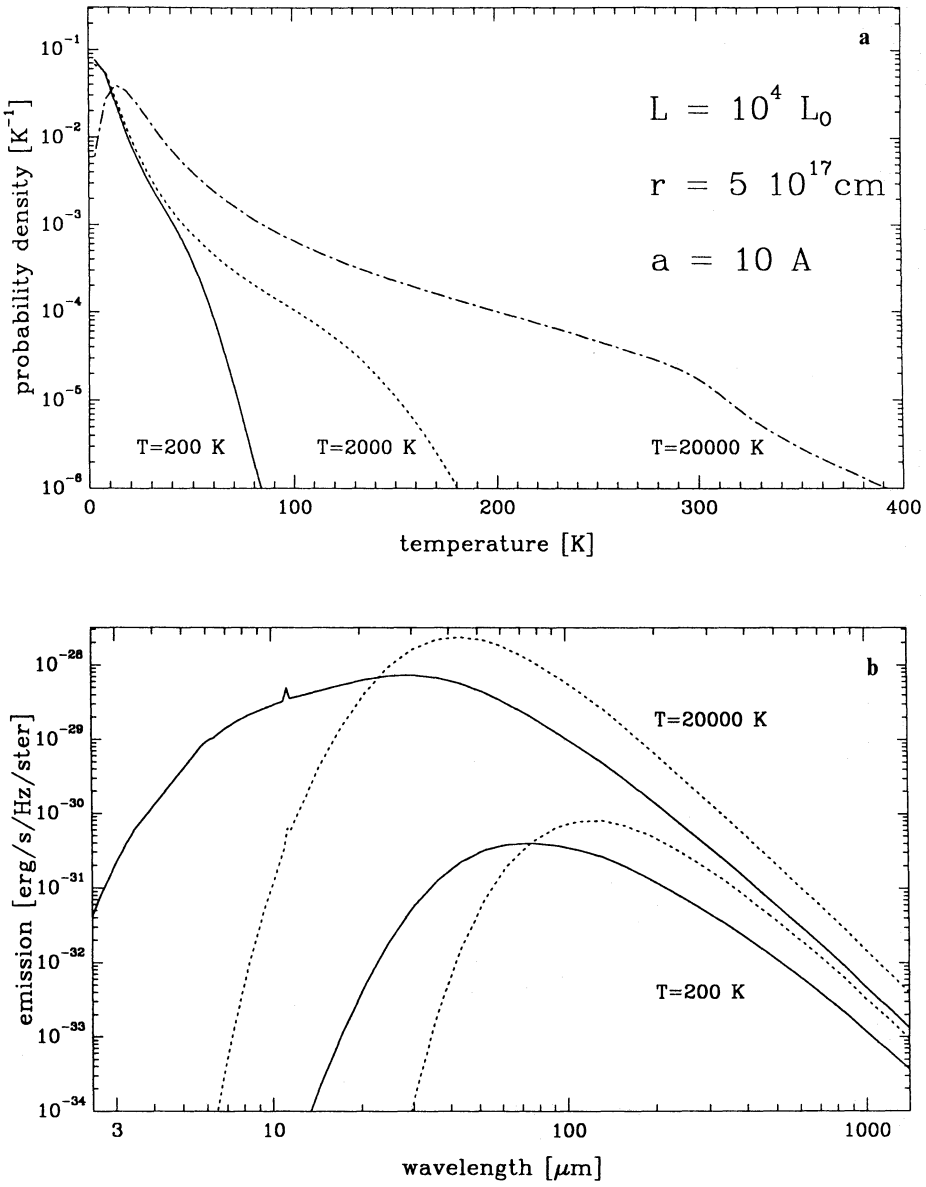

Fig. 5a and b. Same as Fig. 4, but now for a grain radius of only 10 Å

temperature $T(t)$. After the absorption of an energetic photon the grain is heated to a peak temperature T_P (Leger & Puget 1984). It is assumed that this is an infrequent event so that the grain has enough time to cool to an equilibrium state, determined by a background of soft photons with mean intensity J_ν, before the arrival of the next energetic photon. This simplification is reasonable for the small PAHs. The particle emission then follows from a slight modification of Eq. (1)

$$4\pi \int K_\nu J_\nu \, d\nu - c(T) \frac{dT}{dt} = 4\pi \int K_\nu B_\nu(T(t)) \, d\nu. \quad (5)$$

$c(T)$ denotes the specific heat, the absorption term $4\pi \int K_\nu J_\nu \, d\nu$ is constant in time, i.e. the background radiation field J_ν does not contain energetic photons. One may form from the solution of Eq. (5) for $T(t)$ with the starting condition $T(t=0) = T_P$ time averages of $K_\nu B_\nu(T(t))$ (over the interval between the absorption of two energetic photons) and thus evaluate the mean emission. This approach is due to Leger & Puget (1984). Besides the fact that it does not allow multiple energetic photon events it is also very time consuming. However, if the cooling behavior $T(t)$ is known, not necessarily precisely, but only approximately, the method can become very efficient. For example, Allamandola et al. (1989) calculate the cooling rate for the PAH chrysene in a quantum statistical approach. Adapting their results Siebenmorgen (1991) suggests

$$T(t) = (T_P^{-0.4} + \alpha \, t)^{-2.5} \quad (6)$$

with $\alpha \simeq 0.005$. Comparing now the fast GD algorithm for PAHs using 100 enthalpy grids with $T(t)$ given by Eq. (6) we find good agreement in the spectra (Fig. 8), but the latter approach is one order of magnitude faster. Usually the cooling behavior after (Eq. 6) is not strictly correct, i.e. it is not in agreement with the thermal properties of the grain and violates the energy equation. Such inconsistencies can however, be remedied by simply normalizing the emission ε_ν so that ε_ν averaged over time and integrated over frequency equals the total absorbed energy. The final spectrum is then still in very good agreement with the results from calculations after GD.

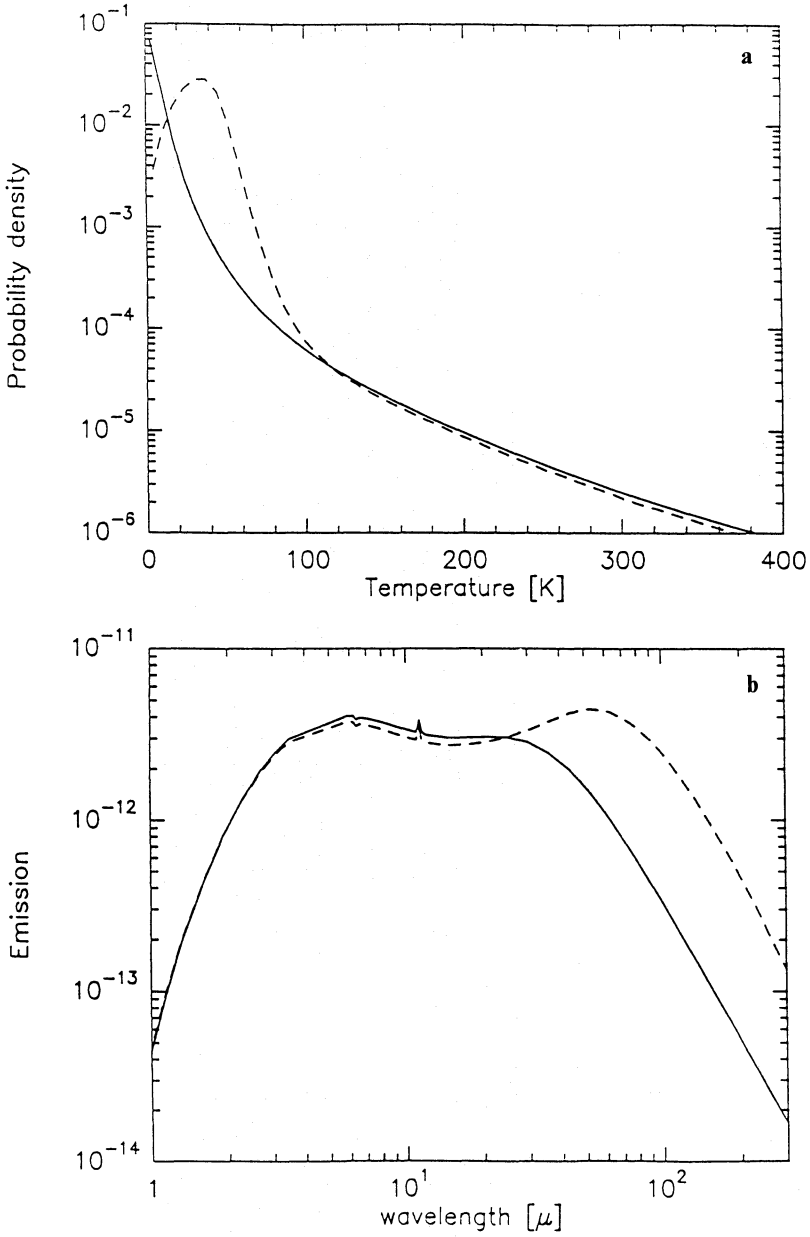

Fig. 6a and b. The emission ε_ν and probability function $P(T)$ of a graphite grain with 5 Å radius located 5 10^{17} cm away from a B1V star is calculated after Eqs. (3) and (4) in two ways. First, assuming that emission occurs only from an initial state i to the next lower $f = i-1$. Then the transition probabilities A_{fi} are zero for $f > i+1$ (solid line) and Eq. (4) can be solved by a fast algorithm (GD). Second, allowing downward transitions from i to any $f > i$ (dashed). Now the full matrix A_{fi} has to be inverted and computation is much more time consuming. For $\lambda \leqq 40\,\mu$m the two methods give very similar results, but in the submm region they differ by orders of magnitude

So far it has always been assumed that Kirchhoffs's law is valid, i.e. at any given instant $\varepsilon_\nu = K_\nu B_\nu(T)$. However, for particles consisting of only a few atoms the cooling should not be treated classically, but in the microcanonical approximation. This is discussed by Barker & Cherneff (1989) and d'Henedourt et al. (1989). They find that, at least for the higher temperatures (> 150 K) the canonical (thermal) approximation is acceptable.

3. Very small silicate grains

It is usually assumed that the small grains with temperature fluctuations are made of carbon. First, because the 2175 Å bump in the extinction curve with its very constant center wavelength is best explained by small (< 100 Å) graphites (Draine 1989) and, second, because the near and mid IR resonances seen in emission in reflection nebulae and other sources are well interpreted by PAHs of 5–10 Å in diameter. One may therefore wonder if not some silicates, which form the other major constituent of interstellar dust, should also exist in the form of equally tiny particles.

So far there has been no need to invoke them as most observations are not sensitive to the lower limit a_1 of the grain size distribution. For grains much smaller than the wavelength (Rayleigh limit) the mass coefficient for extinction, $K_{ext} = K_{abs} + K_{sca}$, becomes independent of the size of the particles. The absorption and scattering coefficient depend then only on the grain volume: $K_{abs} \propto volume$ and $K_{sca} \propto (volume)^2$, scattering being usually negligible. Therefore the extinction curve cannot be used to gain information on a_1.

In the absence of other spectral signatures very small silicate grains might be recognized by their emission in the Si–O stretching vibration at 10 μm. We assume that despite their minute size they are still made up of the characteristic silicate building blocks, i.e. a silicon atom located in a tetrahedron of oxygen

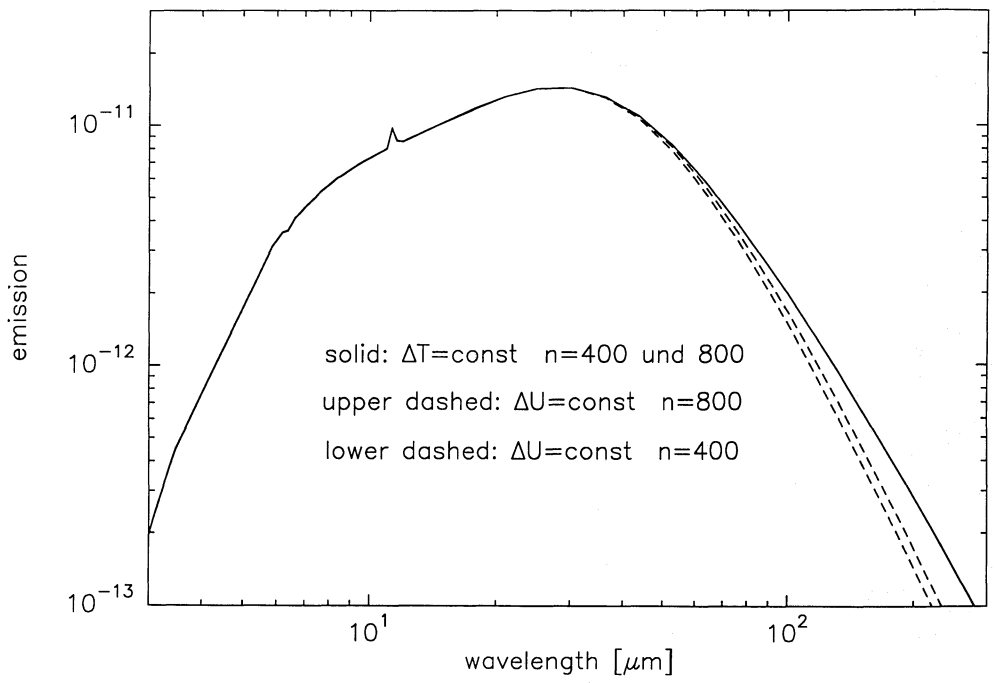

Fig. 7. The emission of a graphite grain with 10 Å radius located $5\ 10^{17}$ cm from a B1V star is calculated after Eqs. (3) and (4) with a vector P_i of size 400 and 800, respectively. The dashed lines show the spectra assuming enthalpy bins of constant width ΔU, the solid line when ΔT = const.; here the results for a vector size of 400 and 800 are identical. Although the energy equation is in both cases fulfilled to better than 1% there are discrepancies in the far IR. As the two dashed lines converge against the solid line we recommend a binning with ΔT = const.

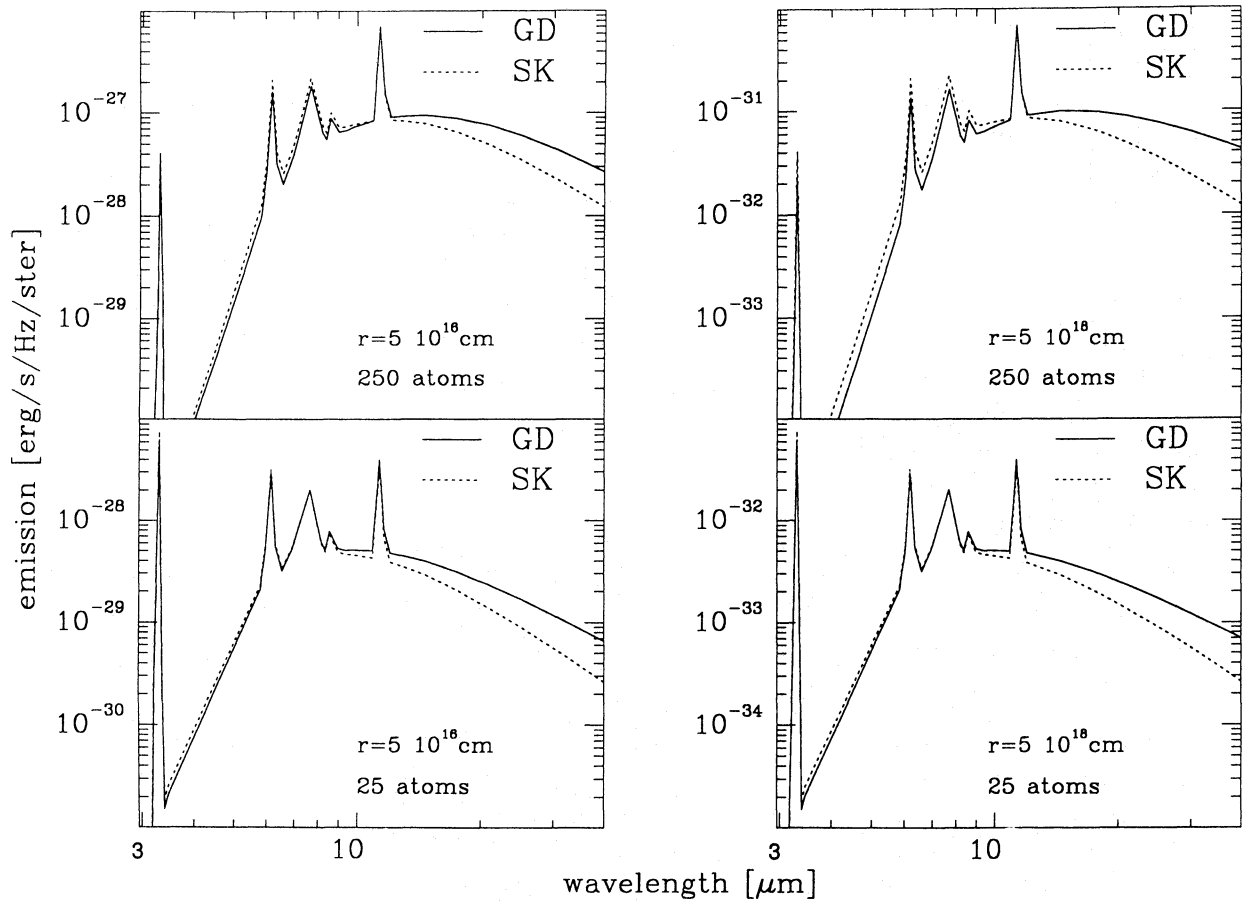

Fig. 8. A comparison of two methods for calculating the emission from PAHs: solid line after GD (Eqs. 3 and 4), dashed line assuming a cooling behavior after Eq. (6). In the latter method, which is much faster, the emission $\varepsilon_\nu(t) = K_\nu\ B_\nu(T)$ is averaged over the time interval between the absorption of two energetic photons and normalized so that the energy equation is strictly fulfilled. The spectra are plotted for PAHs with 25 and 250 carbon atoms at a distance of $5\ 10^{16}$ and $5\ 10^{18}$ cm from a B1V star

atoms. The emissions of the very small and large silicate grains are distinct if there is a hard, but diluted radiation field such that the large grains stay too cold to show the 10 μm Si – O feature, while the very small ones, transiently heated to high temperatures, emit it.

A favourable environment where very small silicate grains may produce a detectable 10 μm feature is a reflection nebula. Let it have an illuminating star of spectral type B1V with $L = 10^4 L_\odot$ and $T_* = 20000$ K. A dust model that successfully explains the extinction curve and IR emission of reflection nebulae, including PAH features, was presented by SK (see also Desert et al. 1990). We briefly mention the salient features of the dust model for use in Sect. 5. There are three dust populations: (i) Big grains ($a > 100$ Å) of amorphous silicate and glassy carbon with a power law size-distribution $n(a) \propto a^{-q}$, $q = 3.5$, that are responsible for the FIR emission and the linear rise in the extinction curve. (ii) Small graphites with a power law size distribution between 5 to 80 Å of exponent $q = 4$ explain the 2175 Å extinction bump and produce the mid IR emission. They undergo temperature fluctuations. (iii) PAHs of two sizes: small ones with $N_c \simeq 25$ and so called clusters with $N_c \simeq 250$. They account for the continuum in the near and, partially, mid IR emission as well as for the sharp resonances in this region. Furthermore, they are responsible for the non-linear rise of the extinction curve in the far UV. PAHs, too, undergo temperature fluctuations. For the calculation of the cross sections, the data base for the optical and thermal grain properties one may consult SK.

For the 10 μm feature in a reflection nebula to be unambigously attributable to very small grains requires that the temperatures of the big amorphous silicates stay below $\simeq 100$ K. Then they radiate only weakly in the 10 μm region and do not swamp the emission of the very small grains. This condition implies distances to the star $r \geqq 2\ 10^{17}$ cm. If we, rather conservatively, assume that the population of very small silicates is in abundance and sizes similar to that of the very small graphites (i.e. they make up 10% of the total silicate material, have radii from 5 to 80 Å and a size distribution $n(a) \propto a^{-4}$) then their emission at a distance of 10^{18} cm to the star is shown in Fig. 9a together with the contribution from the other dust components. Their 10 μm emission is very strong, but competes with the very small graphites and partly with the 11.3 μm PAH resonance. Nevertheless, in the total spectrum one can clearly discern it. For a more extreme, but still not unplausible situation one would make the small silicates still smaller and increase their abundance relative to that of the small graphites. An example is given in Fig. 9b. The dust parameters are summarized in Table 1.

The corresponding observations should be performed as absolute flux measurements or with a large chopper throw so that the off-beam is well outside the nebula. From an analysis of the observations in the 10 μm region in N 2023 and N 7023 (SK) one can conclude that the fraction of silicate material in very small particles is 5% or less, provided particle radii range from 5 to 80 Å, or they are on the average somewhat larger than 10 Å. A similar result was obtained by Desert et al. (1986b).

Table 1. Parameters of dust components, the notation refers to SK

Parameter	Notation	N 2023	Globule
Amorphous carbon			
Lower size	a_-^{ac} (Å)	300	300
Upper size	a_+^{ac} (Å)	1200	1200
Amorphous silicate			
Lower size	a_-^{as} (Å)	300	300
Upper size	a_+^{as} (Å)	2400	2400
Small graphite			
Lower size	a_-^{sg} (Å)	5	10
Upper size	a_+^{sg} (Å)	80	80
Abundance	$Y_C^{sg}(10^{-5})$	(a) 4.5 (b) 1.5	5
Small silicate			
Lower size	a_-^{ss} (Å)	5	?
Upper size	a_+^{ss} (Å)	(a) 80 (b) 20	?
Abundance	$Y_{si}^{ss}(10^{-5})$	0.31	?
Small PAH			
Abundance	$Y_C^{PAH}(10^{-5})$	0.061	2
H/C atom ratio	$\alpha_{H/C}^{PAH}$	0.05	0.2
PAH clusters			
Number of C atoms	N_c^{clu}	140	250
Abundance	$Y_C^{clu}(10^{-5})$	0.28	3
H/C atom ratio	$\alpha_{H/C}^{clu}$	0.2	0.2

4. The radiative transfer including small grains

For the solution of the equation of radiative transfer in spherical geometry we follow the ray tracing method developed by Hummer & Rybicky (1971). Let $I_\nu^+(p,z)$ and $I_\nu^-(p,z)$ be the intensity in positive and negative z-direction, where $z = r\cos(\mu)$ and $p = r\sin(\mu)$. Defining

$$u(p,z) = 0.5 \cdot (I^+(p,z) + I^-(p,z)) \tag{7}$$

one derives the transfer equation

$$\frac{1}{K^t}\frac{\partial}{\partial z}\left(\frac{1}{K^t}\frac{\partial u}{\partial z}\right) = u_\nu - \frac{K^{sca}}{K^t} J_\nu - S_\nu. \tag{8}$$

The boundary condition at the outer edge (cloud radius R) is

$$\frac{1}{K^t}\frac{\partial u}{\partial z} + u = I_0 \text{ for } z = (R^2 - p^2)^{1/2} \tag{9a}$$

and at the inner edge

$$\frac{1}{K^t}\frac{\partial u}{\partial z} = 0 \qquad \text{for } z = 0 \tag{9b}$$

If the cloud is heated by a central star of radius r_* then the inner boundary condition is replaced for $p < r_*$ by

$$-\frac{2}{K^t}\frac{\partial u}{\partial z} = B_\nu(T_*) \tag{9c}$$

I_0 is the intensity of the radiation field impinging from outside, T_* the effective temperature of the star, S_ν the source function. K_ν^t, K_ν^{sca} and K_ν are the cross sections for extinction, scattering and absorption, respectively. J_ν denotes the zeroth, H_ν the first moment of the intensity. The latter are derived from u_ν according to

$$v(p,z) = -\frac{1}{K^t}\frac{\partial u}{\partial z} \tag{10}$$

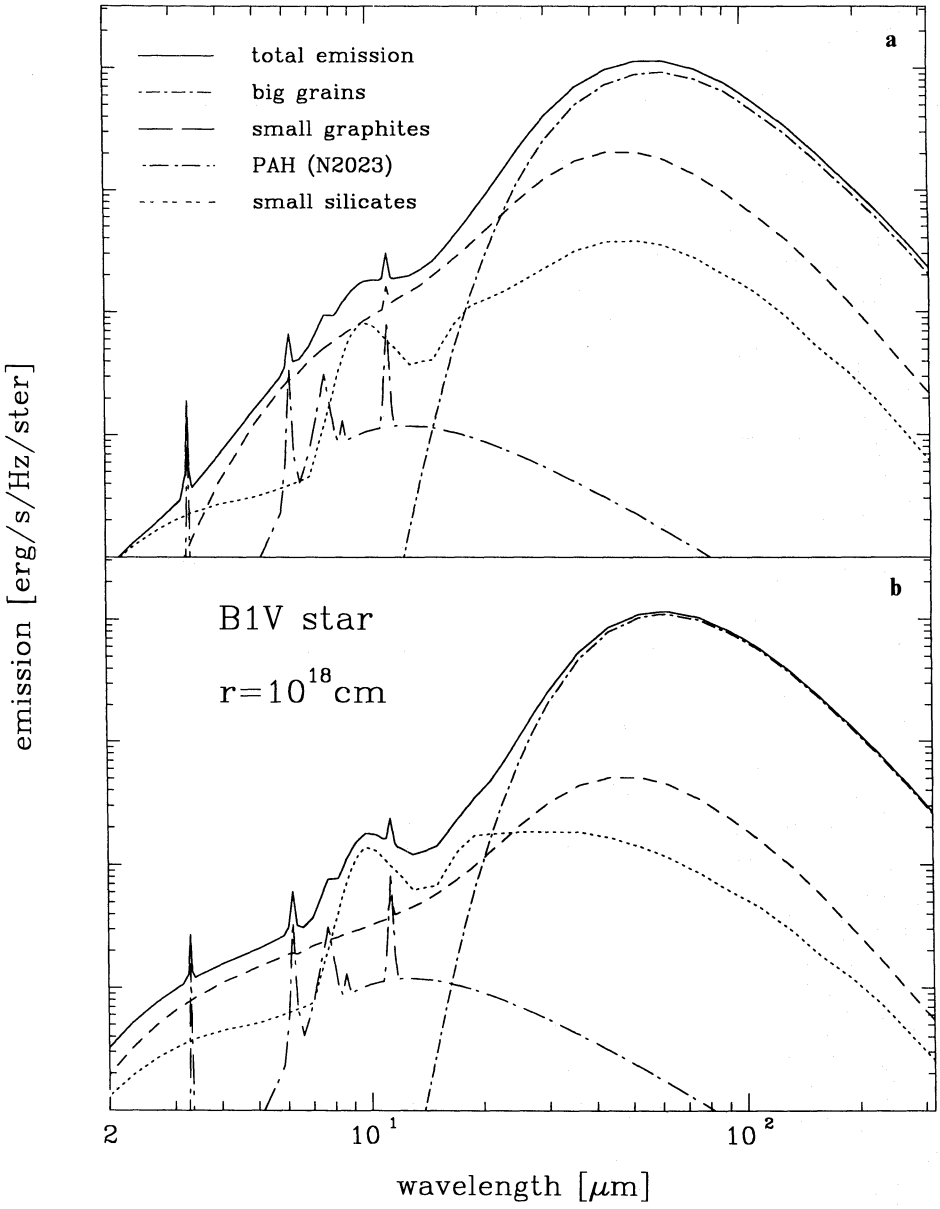

Fig. 9a and b. We investigate whether very small silicate grains can be detected by their 10 μm emission feature. The figures show the emission from dust in a reflection nebula located 10^{18} cm from the central B1 V star. The ordinate (logarithmic scale) is arbitrary and proportional to the column density. Parameters for the big grains and the PAHs are taken from the fit to N 2023 by SK. **a** and **b** are for two sets of dust parameters that are listed in Table 1

$$H_\nu(r)\, r^2 = \int_0^r \mathrm{d}p\, p\, v(p,r) \tag{11}$$

$$J_\nu(r)\, r = \int_0^r \frac{p\, u(p,r)\, \mathrm{d}u}{(r^2-p^2)^{1/2}} \tag{12}$$

As Eq. (8) is valid only for isotropic scattering we replace the scattering efficiencies $Q_\nu^{\mathrm{sca}}(a)$ by $(1-g_\nu)\, Q_\nu^{\mathrm{sca}}$, where a is the grain radius and $g_\nu(a)$ the asymmetry factor. Q_ν^{sca} and g_ν are calculated from Mie theory. There are three dust populations: PAHs, small graphites and big grains. Only the latter contribute to the scattering. Therefore K^{sca} is given by summing over all big particles which differ in size as well as composition (amorphous carbon or silicate):

$$K^{\mathrm{sca}} = \sum_i \pi a_i^2\, (1-g_i)\, Q_i^{\mathrm{sca}} \tag{13}$$

For absorption small graphites and PAHs may not be neglected. The emission of the big grains at equilibrium temperature T_{eq} may be written as

$$\varepsilon_\nu^{\mathrm{big}} = \sum_i K_\nu^{\mathrm{big}}(a_i)\, B_\nu(T_{\mathrm{eq}}(a_i)) \tag{14}$$

For the small graphites (sg)

$$\varepsilon_\nu^{\mathrm{sg}} = \sum_i K_\nu^{\mathrm{sg}}(a_i) \int B_\nu(T)\, P(T) \tag{15}$$

An analogous expression is obtained for the PAHs. Consequently,

$$S_\nu = \frac{\varepsilon_\nu^{\mathrm{big}} + \varepsilon_\nu^{\mathrm{sg}} + \varepsilon_\nu^{\mathrm{PAH}}}{K_\nu^{\mathrm{sca}} + K_\nu^{\mathrm{big}} + K_\nu^{\mathrm{sg}} + K_\nu^{\mathrm{PAH}}} \tag{16}$$

In a zeroth approximation we neglect the small graphites and PAHs, put $J_\nu = 0$ and solve Eq. (8) for u_ν with some estimate for

the temperature of the big grains $T_{eq}(a,r)$. From this first solution for $u_\nu(p,r)$ we calculate $J_\nu(r)$ and from J_ν the emission coefficients ε_ν^{big}, ε_ν^{sg}, ε_ν^{PAH} and thus the full source function S_ν (Eq. 13). Solving Eq. (8) again for u_ν we obtain now improved values of J_ν and S_ν. This procedure is iterated until the total flux $4\pi r^2 \int H_\nu(r)\,d\nu$ has converged either towards the luminosity of the embedded star or towards zero in the case of a cloud without inner sources. Usually five iterations are sufficient. We typically use 50 radial grid points, as many directions (impact parameter p), 100 frequencies, 200 enthalpy bins for the very small grains, 5 different radii for the very small graphite grains and two kinds of PAHs. There are additionally 6 different sizes of the large silicate and amorphous carbon grains. Because the quantum heating problem has to be solved very often in a radiative transfer calculation ($5 \times 50 \times 7$ times) it is evident that one needs a quick algorithm for determining the distribution function $P(T)$.

5. Globules

Very small grains are an inconspicous component in terms of mass, but they can have a dramatic effect on the dust radiation. For instance, in the diffuse intercloud medium of the solar neighborhood their emission dominates at all near and mid IR wavelengths up to 60 μm (SK). Therefore one may expect that their presence also significantly changes the spectrum of compact isolated clouds devoid of embedded stars that are heated from outside by the interstellar radiation field (ISRF). Such clouds, often called globules, are usually not transparent to stellar photons. This is evident from the empty patches they form on the Palomar Sky Survey plates. Consequently, their spectra must be computed via a radiative transfer in the cloud. We investigate their emission and assume a spherical globule of constant density and diameter $2R = 10^{18}$ cm corresponding to $\simeq 2'$ at the distance of Orion. We vary the visual extinction from the surface to the center of the cloud between 3 and 30 mag, the globule mass is then about 6 and 60 $M_\odot$, respectively, and we perform calculations for two radiation fields. First, for the ISRF with a mean intensity J_ν^{ISRF} after Perault et al. (1989), which yields after integration over frequency $4\pi J = 4\pi \int J_\nu^{ISRF}\,d\nu = 0.036\,erg\,cm^{-2}\,s^{-1}$. ($J_\nu$ from Mathis et al. (1983) gives very similar results) This implies that the cloud receives from the ISRF a luminosity $L = 4\pi R^2\,\pi J = 29\,L_\odot$. Second, for a radiation field that is ten times stronger, i.e. the luminosity through the surface of the globule $L = 290\,L_\odot$. Because such a radiation field may be realized in the vicinity of a hot star we assume an impining intensity $J_\nu = 10^{-14}\,B_\nu(T = 20000\,K)$ for

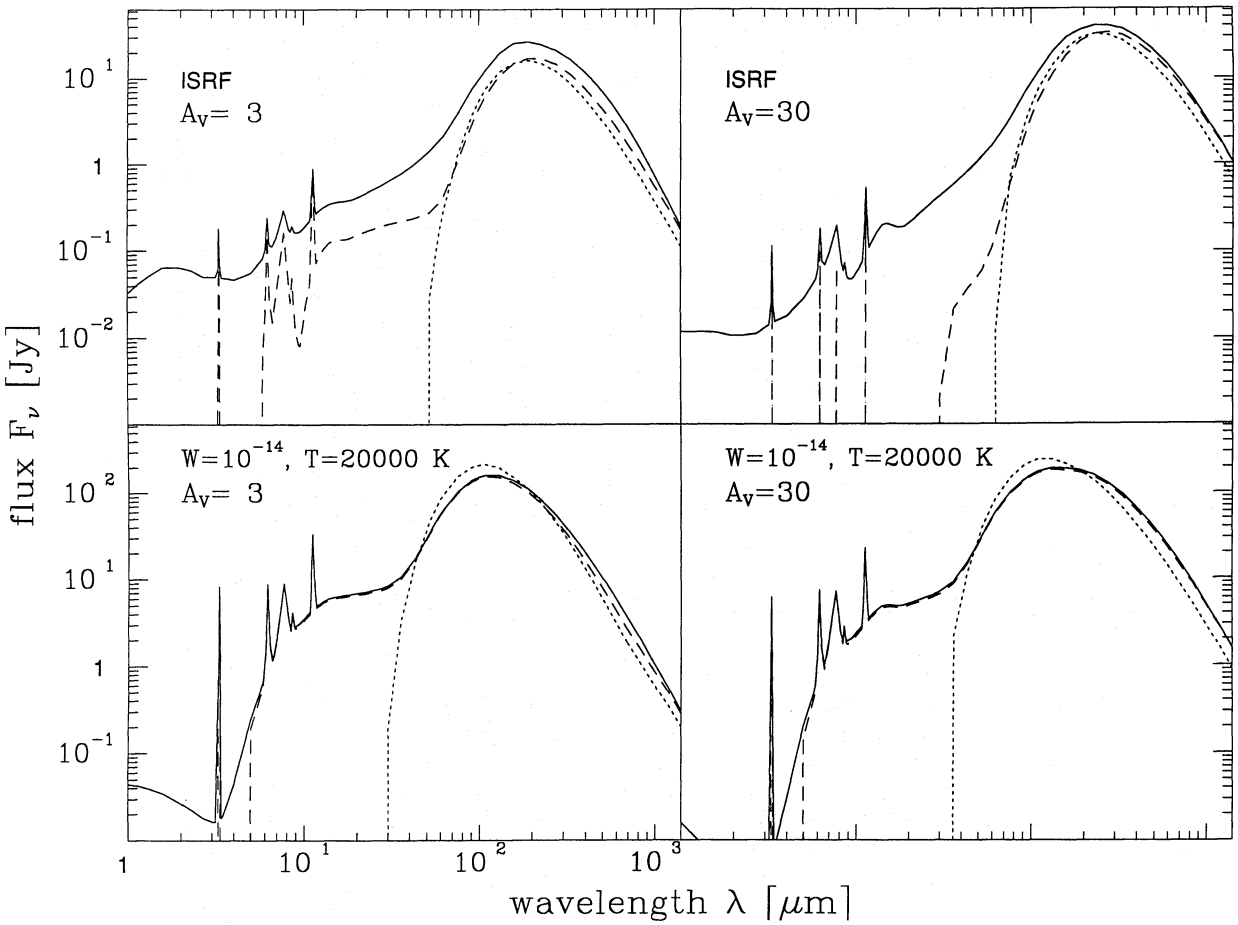

Fig. 10. The emission of an isolated globule without an embedded energy source heated by an outer radiation field which is either the JSRF of the solar neighborhood or its mean intensity is given by $J_\nu = 10^{-14}$, $B_\nu(T = 20000\,K)$. It has a constant density, a radius $R = 5\ 10^{17}$ cm, and an $A_V = 3$ or 30 mag to the cloud center. The globule, at a distance of 500 pc, is observed with a beam larger than the source. The dotted lines give the emission from big grains alone assuming beam switching. For a dust model including very small graphite grains and PAHs the dashed lines show the emission for beam switching and the solid lines depict the absolute fluxes

which $4\pi \int J_\nu \, d\nu = 0.36 \, \mathrm{erg \, cm^{-2} \, s^{-1}}$. Note that an embedded star will show up energetically (i.e. in the far IR) only if it has a luminosity comparable to the flux that flows in from outside, otherwise it may only be detected as a near IR point source. The visual and UV photons are absorbed at the surface of the globule in a layer of optical thickness $\tau_V \simeq 1$. They are converted into IR photons that either leave the cloud or, together with the IR photons of the ISRF, heat the cloud core.

For the dust we use the model similar to that of the solar neighborhod of SK (see Table 1). In Fig. 10 we plot the spectra for a distance of 500 pc obtained with a circular beam of rectangular profile that subtends a solid Ω larger than the source. We show absolute fluxes, like those from IRAS where no off-position has been subtracted, and we simulate the standard observational procedure of beam switching by subtracting the flux $\Omega \, J_\nu^{\mathrm{ISRF}}$, where J_ν^{ISRF} is the outer radiation field.

Let us first consider a dust model consisting only of big grains. Heated by the ISRF, they attain their maximum temperature of 14–19 K at the surface of the globule with $A_V = 3$ mag; deep inside they cool to 11–15 K. Therefore the peak flux occurs at 200 μm and the dust emission itself below 60 μm is very weak. Looking at the globule at these wavelengths, the flux is due to photons of the ISRF that stream in at the backside of the globule and are then attenuated within it so that an observational off-position (blank sky) appears brighter than the on-position (source). ON-minus-OFF becomes negative and in beam switching the spectrum displays a sharp cutoff at $\simeq 60$ μm. This behavior has already been discussed elsewhere (Spencer & Leung 1978; Lee & Rogers 1987; Leung et al. 1989). Whenever intrinsic emission by the source can be neglected absolute fluxes towards it are given by $\Omega \, J_\nu^{\mathrm{ISRF}} \exp(-\tau_\nu)$.

Increasing the optical depth of the globule from $A_V = 3$ to 30 mag, while keeping its outer radius R constant, raises the cloud mass linearly with A_V. As in this case the total heating flux for the globule does not change, it is fixed by $J \, R^2$, each gram of matter receives on the average less energy and the wavelength of maximum emission $\lambda_{\max}$ shifts further to the red ($\simeq 250$ μm). Increasing the strength of the outer radiation field has little effect on the shape of the spectrum for the model containing only big grains.

This picture changes drastically if we include small grains since they dominate the emission for $\lambda < 50$ μm. The cutoff λ_c is now at much shorter wavelengths (Lis & Leung 1991a): for the globule with $A_V = 30$ heated by the ISRF $\lambda_c \simeq 30$ μm and at 5 μm for the other models. For this reason one detects extended emission from globules not only in the far IR but also at mid IR and slightly shorter wavelengths. This emission is observed as IR limb brightening at all four IRAS bands, e.g. in the diffuse cloud G 300-17 (Laureijs 1989), in Barnard 5 (Beichman et al. 1988, Langer et al. 1989) and in other clouds (Chlewicki et al. 1987, 1988). For Barnard 5 Lis & Leung (1991b) cannot explain the observed 12 μm flux solely by small graphites and suggest the missing emission is due to PAHs. In our model most of the 12 μm flux is produced by PAHs. The 25 μm emission mainly comes from small graphites which contribute also to the 60 μm band. The 100 μm emission is given by the large grains. To confirm the existence of PAHs in this class of objects one needs spectral observations in the 3–13 μm region.

For globules heated by the strong radiation field of a nearby B star the spectra obtained with beam switching and from absolute fluxes are almost identical. The situation is very different for the globules heated by the ISRF. Their emission is comparable to the background which leads to dramatic changes when comparing the spectra of a beam switching procedure with absolute fluxes. For example, in the case of the globule with $A_V = 3$ heated by the ISRF, beam switching generates a 9.7 μm silicate feature through the absorption of the smooth 10 μm ISRF background within the globule. The 9.7 μm feature is not due to silicate self absorption as the silicate grains are much too cold ($T_{\mathrm{eq}} < 20$ K) to emit at these wavelengths. On the other hand, the 18 μm silicate absorption is only very weakly seen because its optical depth in the globule is much lower.

As part of the heating flux is absorbed by the small grains the large particles attain a temperature somewhat lower than in the models containing only big grains. This explains the slight differences in the far IR and submm between both dust concepts.

References

Aannestad P.A., Kenyon S.J., 1979, Ap&SS 65, 155
Aitken D.K., 1981, IAU Symp. 96, 207
Allamandola L.J., Tielens A.G.G.M., Barker J., 1989, ApJS 71, 733
Barker J., Cherneff I., 1989, IAU Symp. 135, 197
Beichman C.A., Wilson R.W., Langer W.D., Goldsmith P.F., 1988, ApJ 332, L81
Boulanger F., Perault F., 1988, ApJ 330, 964
Chini R., Krügel E., Kreysa E., 1986, A&A 167, 315
Chlewicki G., Laureijs R.J., Clark F.O., Wesselius P.R., 1987. In: Star Formation in Galaxies, Lonsdale Persson C.J., (eds.), NASA CP-2466, p. 113
Chlewicki G., 1988. In: Experiments on Cosmic Dust Analogues (eds.), Bussoletti E., Fusco C., Longo G. (eds.), Kluwer, Dordrecht, p. 313
Desert F.X., Boulanger F., Shore S.N., 1986, A&A 160, 295
Desert F.X., Boulanger F., Puget J.L., 1990, A&A 237, 215
Desert F.X., Boulanger F., Leger A., Puget J.L., Sellgren K., 1986b, A&A 159, 328
d'Hendecourt L.B., Leger A., Boissel P., Desert F.X., 1989, IAU Symp. 135, 207
Draine B.T., Anderson N., 1985, ApJ 292, 494
Draine B.T., 1989, IAU Symp. 135, 313
Duley W.W., 1973, Ap. Space. Sci. 23, 43
Dwek E., 1986, ApJ 302, 363
Greenberg J.M., Hong S.S., 1974, IAU Symp. 60, 155
Guhathakurta P., Draine B.T., 1989, ApJ 345, 230 (GD)
Hummer D.G., Rybicki G.B., 1971, MNRAS 152, 1
Langer W.D., Wilson R.W., Goldsmith P.F., Beichman C.A., 1989, ApJ 337, 335
Laureijs R.J., 1989, PhD thesis: University of Groningen, 79
Lee M.H., Rogers C., 1987, ApJ 317, 1987
Leger A., Puget J.L., 1984, A&A 137, L5
Leung C.M., O'Brien E.V., Dubish R., 1989, ApJ 337, 293
Lis D.C., Leung C.M., 1991a, ICARUS 91, 7
Lis D.C., Leung C.M., 1991b, ApJ 372, L107
Mathis J.S., Mezger P.G., Panagia N., 1983, A&A 128, 212
Puget J.L., Leger A., 1989, ARAA 27, 161
Purcell E.M., 1976, ApJ 206, 685
Perault M., Boulanger F., Puget J.-L., Falgarone E., 1989, ApJ (submitted)
Sellgren K., 1984, ApJ 277, 623
Siebenmorgen R., 1991, PhD thesis: University of Bonn
Siebenmorgen R., Krügel E., 1992, A&A 259, 614 (SK)
Spencer R.G., Leung C.M., 1978, ApJ 222, 140